Controlling dynamical systems using multiple delay feedback control

Alexander Ahlborn and Ulrich Parlitz
Drittes Physikalisches Institut, Universität Göttingen, Bürgerstraße 42-44, 37073 Göttingen, Germany
(Received 18 November 2004; revised manuscript received 4 March 2005; published 13 July 2005)

Multiple delay feedback control (MDFC) with two, three, or four different and independent delay times is used to stabilize steady states of various chaotic dynamical systems. A comparison with delayed feedback control methods that are based on a single (fundamental) delay time [Pyragas' time delay auto synchronization (TDAS) and extended TDAS] shows that MDFC is more effective for fixed point stabilization in terms of stability and flexibility, in particular for large delay times.

DOI: 10.1103/PhysRevE.72.016206 PACS number(s): 05.45.Gg

I. INTRODUCTION

During the past 15 years many control methods have been suggested for controlling chaos and stabilizing periodic orbits [1–6,8–13]. One of these schemes is the method of Ott, Grebogi, and Yorke (OGY) [2] that is based on local approximations of the Poincaré map in embedding space. This method requires analog/digital (A/D) conversion, numerical computations of the control signal, and subsequent D/A conversion. Therefore, it is very difficult to apply OGY control to fast dynamical systems. Alternatives that enable implementations with analog hardware are *occasional proportional feedback* (OPF) [3,4] or delayed feedback methods that are the main topic of this article. The most well-known delay method is *time delay auto synchronization* (TDAS) [5–7], also known as Pyragas' method, where the control signal is an amplified difference of a suitable observable measured at times t and $t-\tau$. For a controlled system

$$\dot{\mathbf{x}} = \mathbf{f}(\mathbf{x},\mathbf{u}) \tag{1}$$

the TDAS control signal $\mathbf{u}$ may in general be written as

$$\mathbf{u}(t) = k\{\mathbf{g}(\mathbf{x}(t-\tau)) - \mathbf{g}(\mathbf{x}(t))\}. \tag{2}$$

In Eq. (2) $\mathbf{u}$ denotes the feedback signal, k is an appropriate gain factor, and $\mathbf{g}$ defines a measurement function of the system's state $\mathbf{x}$. A generalization of Pyragas' method (TDAS) is *extended time delay auto synchronization* (ETDAS) that was introduced by Gauthier *et al.* in 1996 [8–11]. With ETDAS a (fundamental) delay time τ and its integer multiples $j\tau$ are used to form the ETDAS feedback signal in the form of a geometric sum. Using the same abbreviations as in (2) this control method reads

$$\mathbf{u}(t) = k\left((1-R)\sum_{j=1}^{\infty} R^{j-1}\mathbf{g}(\mathbf{x}(t-j\tau)) - \mathbf{g}(\mathbf{x}(t))\right) \tag{3}$$

whereas $R \in]-1,1[$ is a weighting factor for the geometric sum. In experimental situations ETDAS can be implemented with a single delay line if the corresponding signal passes the delay line several times. In Ref. [10] it is claimed that the optimal parameters for fixed point control are $R \to 1, \tau \to 0$. In this limit ETDAS turns out to be a single pole high-pass filter given by the equation

$$\dot{\mathbf{u}}(t) = -\omega_0\mathbf{u}(t) - k\dot{\mathbf{g}}(\mathbf{x}(t)) \tag{4}$$

with cutoff frequency $\omega_0 = (1-R)/\tau$ and gain factor k.

Another generalization of TDAS is NTDAS (*N time delay auto synchronization*) [12] where the mean value of a finite number of delay terms is used as a control signal. Similar to ETDAS all occurring delay times are integer multiples of some basic delay time τ. This leads to the following NTDAS feedback signal

$$\mathbf{u}(t) = k\left(\frac{1}{N}\sum_{j=1}^{N}\mathbf{g}(\mathbf{x}(t-j\tau)) - \mathbf{g}(\mathbf{x}(t))\right). \tag{5}$$

TDAS and ETDAS can easily be implemented by means of analog electronics [7] and are therefore applicable to fast dynamical systems. Another possibility to control chaos in fast oscillators is a measurement of the system's state at one point in a delay line and applying perturbations at another point [13]. The necessary perturbations are generated by a TDAS controller. With this strategy it was possible to stabilize periodic orbits of an 81 MHz chaotic oscillator [13].

II. MULTIPLE DELAY FEEDBACK CONTROL

Motivated by the task to stabilize the steady state of a frequency-doubled Nd:YAG laser we suggested in Refs. [14,15] a *multiple delay feedback control* scheme (MDFC) based on two or more different delay times which enter independent control terms. In detail we consider the following situation. Given is a vector field $\dot{\mathbf{x}} = \mathbf{f}(\mathbf{x},\mathbf{u})$ to be controlled by the MDFC signal $\mathbf{u}$,

$$\begin{aligned}\mathbf{u}(t) &= k_{1a}\mathbf{g_1}(\mathbf{x}(t-\tau_1)) - k_{1b}\mathbf{g_1}(\mathbf{x}(t)) \\ &\vdots \\ &+ k_{na}\mathbf{g_n}(\mathbf{x}(t-\tau_n)) - k_{nb}\mathbf{g_n}(\mathbf{x}(t))\end{aligned} \tag{6}$$

by means of n different delay times $\tau_1,\ldots,\tau_n$ where the functions $\mathbf{g_i}$ represent the way the feedback is implemented (measurement functions) and the parameters k_{ia}, k_{ib} are used to vary the strength and influence (gain) of the different feedback terms. In contrast to ETDAS or NTDAS these delay times are not integer multiples of each other. Therefore, the feedback signal (6) only vanishes in the case of a steady state [in contrast to (E)TDAS where this happens already for pe-

riodic orbits whose period is an integer multiple of τ]. If an unstable fixed point of the given system [i.e., $\dot{\mathbf{x}}=\mathbf{f}(\mathbf{x})=\mathbf{0}$] is to be stabilized (noninvasive control), the gain factors have to fulfill the additional constraints $k_{1a}=k_{1b},\ldots$ and $k_{na}=k_{nb}$ in the case of different measurement functions. Otherwise a new steady state may be created that is not a fixed point of the vector field $\mathbf{f}$ (but perhaps also interesting for some applications). If the same measurement function $\mathbf{g}(\mathbf{x}(\mathbf{t}))$ is used for all delay times the constraint for noninvasive control reads $\Sigma_{i=1}^{n} k_{ia}-k_{ib}\stackrel{!}{=}0$.

For many dynamical systems it turned out that Pyragas' TDAS method (and its extensions) is very succesful for stabilizing unstable periodic orbits (UPOs) but less effective in terms of stability to control unstable steady states. Therefore, we tested MDFC for several well-known dynamical systems using linear stability analysis of the resulting control problem.

III. LINEAR STABILITY ANALYSIS

The starting point of the linear stability analysis of MDFC control is a given vector field $\dot{\mathbf{x}}=\mathbf{f}(\mathbf{x})$ with a fixed point at $\mathbf{x}_0$. In the following we shall consider an additive control force

$$\dot{\mathbf{x}}(t)=\mathbf{f}(\mathbf{x}(t))+\mathbf{u}(t), \tag{7}$$

where the control signal $\mathbf{u}$ is given by Eq. (6) with gain factors $k_{ia}=k_{ib}=k_i$, $i=1,\ldots,n$. In order to perform a linear stability analysis we are interested in the temporal evolution of small perturbations $\mathbf{e}(t)=\mathbf{x}(t)-\mathbf{y}(t)$,

$$\dot{\mathbf{e}}(t)=\mathbf{f}(\mathbf{x})-\mathbf{f}(\mathbf{y})+\sum_{i=1}^{n} k_i\{\mathbf{g_i}(\mathbf{x}(t-\tau_i))-\mathbf{g_i}(\mathbf{x}(t))\} - k_i\{\mathbf{g_i}(\mathbf{y}(t-\tau_i))-\mathbf{g_i}(\mathbf{y}(t))\}. \tag{8}$$

Linearization yields

$$\dot{\mathbf{e}}(t)=D\mathbf{f}(\mathbf{x})\mathbf{e}(t) + \sum_{i=1}^{n} k_i\big(D\mathbf{g_i}(\mathbf{x}(t-\tau_i))\mathbf{e}(t-\tau_i)-D\mathbf{g_i}(\mathbf{x}(t))\mathbf{e}(t)\big), \tag{9}$$

where $D\mathbf{f}$ and $D\mathbf{g_i}$ denote Jacobian matrices. An ansatz for a general solution of this system is

$$\mathbf{e}(t)=e^{-\lambda t}\mathbf{e}_0,$$

$$\mathbf{e}(t-\tau_i)=e^{-\lambda\tau_i}\mathbf{e}(t). \tag{10}$$

Substituting (10) in (9) and linearizing at the fixed point $\mathbf{x}_0$ yields

$$\dot{\mathbf{e}}(t)=[D\mathbf{f}(\mathbf{x}_0)+U_R(\mathbf{x}_0)]\mathbf{e}(t) \tag{11}$$

with the matrix

$$U_R(\mathbf{x}_0)=\sum_{i=1}^{n} k_i(e^{-\lambda\tau_i}-1)D\mathbf{g_i}(\mathbf{x}_0). \tag{12}$$

The Jacobian matrix $D\mathbf{f}(\mathbf{x}_0)$ in (11) is relevant for the linear stability analysis of the unperturbed system. The feedback signal (6) is taken into account by the second matrix $U_R(\mathbf{x}_0)$. For delay systems the eigenvalue problem of the Jacobian $D\mathbf{f}$ is replaced by the eigenvalue problem of the matrix $D\mathbf{f}(\mathbf{x}_0)+U_R(\mathbf{x}_0)$ in terms of the characteristic matrix [16]

$$\Delta(\lambda)=\lambda I-D\mathbf{f}(\mathbf{x}_0)-U_R(\mathbf{x}_0) \tag{13}$$

and its determinant $\det[\Delta(\lambda)]$ (I denotes the unit matrix). The fixed point $\mathbf{x}_0$ is stable if all roots (eigenvalues) λ of the characteristic equation

$$\det[\Delta(\lambda)]=0 \tag{14}$$

possess negative real parts $\mathrm{Re}(\lambda)$. So, what we need to determine the stability of the controlled system is the eigenvalue with the largest real part. This eigenvalue decides whether the feedback is successful or not. However, since (7) is an infinite-dimensional system and Eq. (14) is a transcendental equation, an infinite number of roots exist which makes this eigenvalue problem more difficult than that of the uncontrolled system. On the other hand, it can be proven [16] that there are only a finite number of roots whose real part is larger than a given constant (for example, larger than zero). In order to find the roots of the characteristic equation we first use a grid in the complex plane to find those points, where the real and the imaginary parts of $\det[\Delta(\lambda)]$ are simultaneously as close as possible to zero. These points are then initial values for a damped Newton's algorithm for the exact calculation of the roots.

Of course, this linear analysis describes only local stability properties. If the controlled dynamical system possesses more than one (stabilized) fixed point, different basins of attraction occur and it depends on initial conditions and all relevant (control) parameters to which of the steady states the (controlled) system converges.

IV. NUMERICAL RESULTS

A. Rössler system

Our first example is the Rössler system,

$$\dot{x}=-y-z,$$

$$\dot{y}=x+ay+u(t),$$

$$\dot{z}=b+(x-c)z, \tag{15a}$$

where MDFC (6) is applied using a control signal $\mathbf{u}=[0,u(t),0]$ with four delay terms and pairwise equal gains $k_{ia}=k_{ib}=k_i$,

$$u(t)=k_1[y(t-\tau_1)-y(t)]+k_2[y(t-\tau_2)-y(t)] + k_3[y(t-\tau_3)-y(t)]+k_4[y(t-\tau_4)-y(t)], \tag{15b}$$

depending and acting on the y variable. Since we are inter-

ested in controlling chaotic systems the chosen parameters for numerical studies are $a=0.2$, $b=0.2$, and $c=5.7$. For these parameter values the free running system ($u=0$) shows the known chaotic motion which is mainly characterized by an unstable spiral in the x-y plane and occasional bursts in the z dimension. The fixed point we want to stabilize is located at the coordinates $\mathbf{x}_0=(x_0,y_0,z_0)=(-as,s,-s)$ with

$$s=-\frac{c}{2a}+\sqrt{-\frac{b}{a}+\left(\frac{c}{2a}\right)^2}.$$

With the feedback signal Eq. (15b) the matrix U_R for the linear stability analysis reads

$$U_R=\begin{pmatrix}0 & 0 & 0\\ 0 & u_R & 0\\ 0 & 0 & 0\end{pmatrix} \tag{16}$$

with

$$u_R(\lambda)=k_1(e^{-\tau_1\lambda}-1)+k_2(e^{-\tau_2\lambda}-1)+k_3(e^{-\tau_3\lambda}-1)+k_4(e^{-\tau_4\lambda}-1). \tag{17}$$

The resulting characteristic matrix

$$\Delta(\lambda)=\begin{pmatrix}\lambda & 1 & 1\\ -1 & \lambda-a-u_R(\lambda) & 0\\ -z_0 & 0 & \lambda-x_0+c\end{pmatrix} \tag{18}$$

leads to the following characteristic equation:

$$\det[\Delta(\lambda)]=[\lambda-a-u_R(\lambda)][z_0+\lambda(\lambda-x_0+c)]+\lambda-x_0+c\stackrel{!}{=}0. \tag{19}$$

As pointed out before, the main task is to find the roots of the transcendental equation (19). The following stability plots have been calculated by linearizing the system equations at the desired fixed point and by computing the relevant roots λ of the characteristic equation (19) for a grid of τ_1 and τ_2 values. Figure 1(a) shows the resulting stability diagram in the τ_1-τ_2 plane for the case of only two delay times ($k_3=k_4=0$) and fixed values of the coupling ($k_1=k_2=0.2$). Regions where a successful stabilization of the system's steady state $\mathbf{x}_0$ is possible are marked black. As can be seen, no TDAS stabilization is possible for $\tau_1=\tau_2>10$, whereas a stabilization of the equilibrium by means of MDFC is possible for much larger values of the delay time (black stripes in parallel to the diagonal) [19]. Since Fig. 1(a) does not provide any information about the quality and robustness of the achieved stabilization we have plotted in Fig. 1(b) $\max[0,-\mathrm{Re}(\lambda)]$ vs τ_1 and τ_2 where λ denotes the root with the largest real part $\mathrm{Re}(\lambda)$. The higher the peaks of this stability function the more stable is the applied feedback. Note that in Fig. 1(b) one looks in the direction of the origin along the diagonal, i.e., this diagram is rotated with respect to Fig. 1(a). To compare MDFC with TDAS and ETDAS, stability diagrams for these control methods are shown in Figs. 1(c) and 1(d) and Figs. 1(e) and 1(f), which have been computed by replacing Eq. (17) by

$$u_R=k\left(\frac{e^{-\tau\lambda}-1}{1-Re^{-\tau\lambda}}\right). \tag{20}$$

ETDAS stabilization in Figs. 1(e) and 1(f) was achieved for $R=0.7$ and led to an enlargement of the stability regions compared to TDAS [$R=0$, Figs. 1(c) and 1(d)]. However, the fixed point is only weakly stable for $\tau>6$ and therefore the stability regions at $\tau\approx 9, \tau\approx 16$, and $\tau\approx 22$ in Figs. 1(c) and 1(e) are almost invisible in the gray-scaled diagrams shown in Figs. 1(d) and 1(f). Higher stability was achieved with ETDAS in the limit $R\to 1, \tau\to 0$ where control with the high-pass filter (4) provided similar results (in terms of real parts of eigenvalues) as MDFC.

In general, fixed point stabilization using MDFC becomes more effective (stable) when using more than two different delay times (with suitably chosen gains and delay times). Figure 2 shows stability diagrams in the τ_1-τ_2 plane for fixed point stabilization based on two and three delay times (for fixed gain factors $k_1=k_2=k_3=0.5$). As can be seen the (black) regions of stability are extended when going from two to three delay times.

One can infer from Figs. 1 and 2 that the stability of feedback is increased by the strength of the gain factors as well as by increasing the number of delay terms with different and suitably chosen delay times. With MDFC and four delay terms it is possible to stabilize the system's steady state with moderate gain factors (e.g., $k_i=0.5$) for any τ_1,τ_2 configuration in the range $0.2<\tau_i<25$ if the other two delay times τ_3 and τ_4 are suitably chosen (for example $\tau_3=5.8$, $\tau_4=1.46$). The horizontal and vertical distance of stripes in parallel to the diagonal in Figs. 1(a) and 2 correspond to one period $T\approx 5.86$ of the system's natural oscillations determined by the first maximum of the autocorrelation function.

If the gain factors in Eq. (15b) are equal (symmetric MDFC), the resulting stability diagram is symmetric with respect to the diagonal in the τ_1-τ_2 plane as can be seen from Figs. 1 and 2. In the case of (only) two delay times this diagonal corresponds to the conventional TDAS (Pyragas) feedback. For asymmetric MDFC feedback the stability diagram loses its symmetry and regions where fixed point stabilization is possible are shifted to the side of higher gain.

To obtain a better insight into the stabilization of fixed points with MDFC we shall now change into the frequency domain. The feedback signal (15b) relates the input signal linearly to the output signal. For (maximal) four independent delay times the corresponding transfer function reads

$$T(\omega)=k_1(e^{-i\omega\tau_1}-1)+k_2(e^{-i\omega\tau_2}-1)+k_3(e^{-i\omega\tau_3}-1)+k_4(e^{-i\omega\tau_4}-1). \tag{21}$$

Examples of this transfer function are shown in Figs. 3(b)–3(d). For comparison the frequency spectrum of the unperturbed Rössler system and the transfer function of the high-pass filter (4) are plotted in Fig. 3(a). In Figs. 3(b) and 3(c) all weights are chosen equally ($k_i=1, \forall i$). The solid line in Fig. 3(b) represents $|T(\omega)|$ for a single delay line with $\tau_1=16.5$ ($k_2=k_3=k_4=0$), the dash-dotted line the result of an additionally applied second delay time of $\tau_2=6$ (active are now $\tau_1=16.5$, $\tau_2=6$, $k_3=k_4=0$). The dotted line shows the

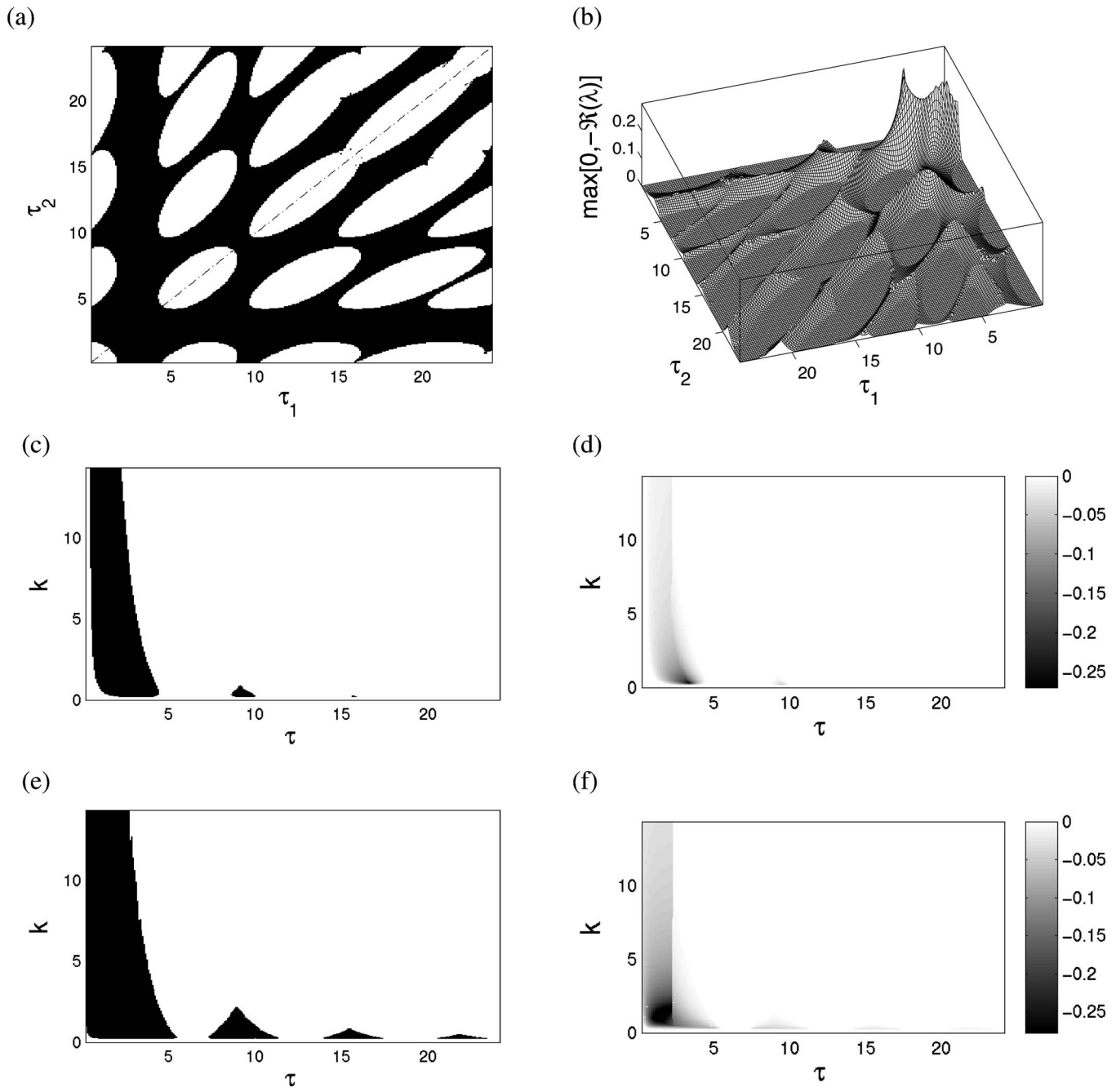

FIG. 1. (a), (b) Stability diagram of the controlled Rössler system (15a) with MDFC (15b) for $k_1=k_2=0.2$, $k_3=k_4=0$. (a) Combinations of delay times τ_1 and τ_2 where MDFC successfully stabilizes the fixed point are plotted in black. (b) Corresponding stability function $\max[0,-\mathrm{Re}(\lambda)]$ vs delay times, where $\mathrm{Re}(\lambda)$ denotes the largest real part of the eigenvalues of the characteristic equation (19). Note that (b) is rotated compared to (a). (c)–(f) Stability diagram for (E)TDAS where the control signal (3) is applied to the Rössler system. (d), (f) Gray-scaled stability function $\min[0,\mathrm{Re}(\lambda)]$ vs τ and k. (c), (d) $R=0$ (TDAS). (e), (f) $R=0.7$ (ETDAS).

consequences of three active delay times chosen as $\tau_1=16.5$, $\tau_2=6$, and $\tau_3=1.5$. Last but not least the effect of four active delay times on $|T(\omega)|$ with $\tau_1=16.5, \tau_2=6, \tau_3=1.5$, and $\tau_4=17.7$ can be obtained from the dashed line. To stabilize a fixed point an appropriate (feedback) filter needs a notch at $\omega=0$ [10]. This frequency (corresponding to a fixed point) is then not fed back to the system in contrast to those frequencies not lying in a notch. With the feedback characteristics shown in Fig. 3(b) (dash-dotted line) stabilization of the system's fixed point is not successful, because this filter has a notch at the characteristic (main) frequency, which is therefore not fed back. In this case it is only possible to generate a new periodic orbit for the perturbed system with nonvanishing feedback signal (invasive control). Only by switching on additionally the third and fourth of the chosen delay times (dotted and dashed line) it is possible to shift and remove notches in the transfer function and to stabilize the considered fixed point. In Fig. 3(c) a choice of delay times is

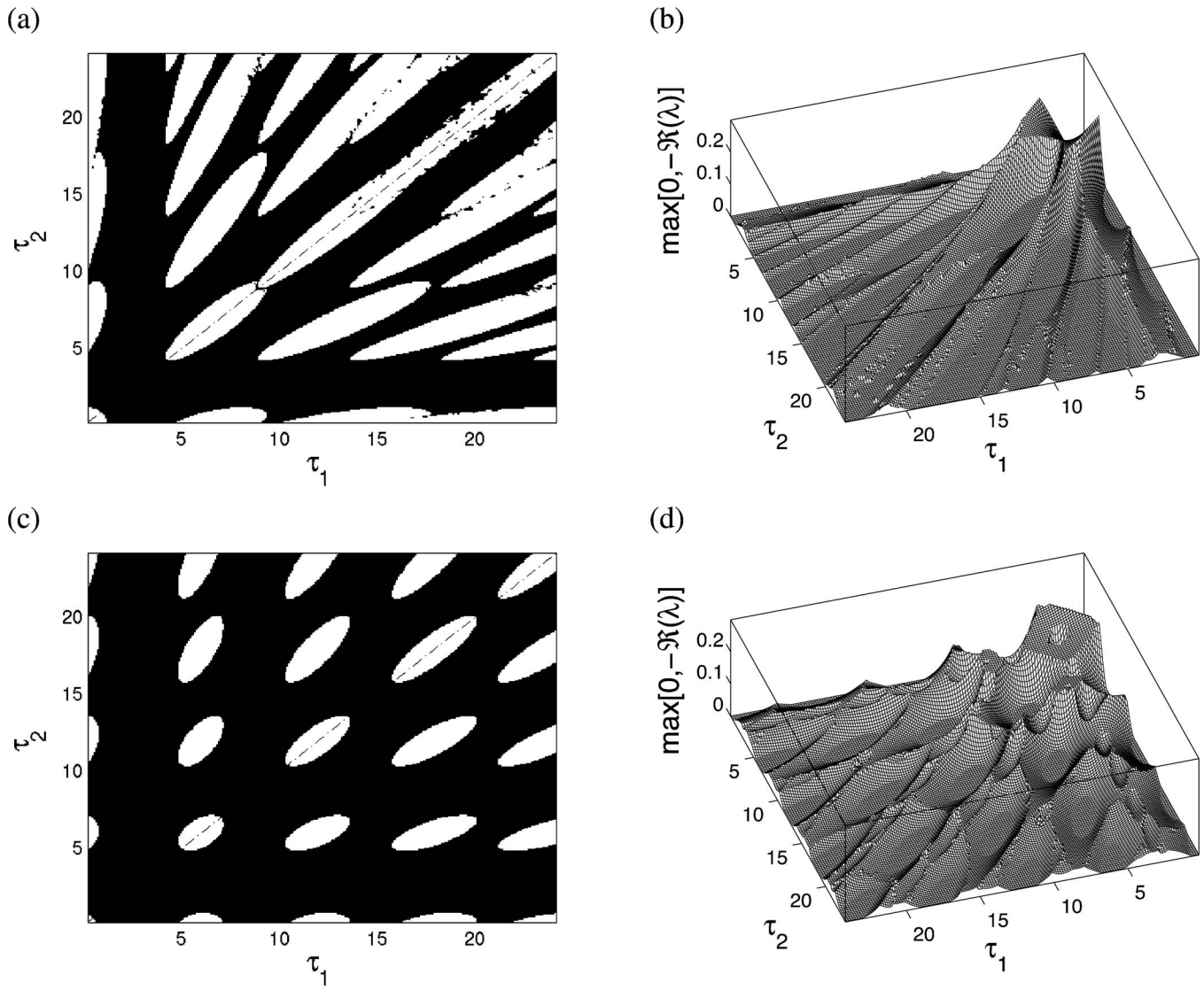

FIG. 2. Stability diagram of the controlled Rössler system (15a) for (a),(b) two delay times ($k_1=k_2=0.5$, $k_3=k_4=0$) and (c),(d) three delay times ($k_1=k_2=k_3=0.5$, $k_4=0$, $\tau_3=5.8$). (a),(c) Combinations of delay times τ_1 and τ_2 where MDFC successfully stabilizes the fixed point are marked in black. (b),(d) Corresponding stability function $\max[0,-\mathrm{Re}(\lambda)]$ vs delay times τ_1 and τ_2. $\mathrm{Re}(\lambda)$ denotes the largest real part of the eigenvalues of the characteristic equation (19). Note that (b) and (d) are rotated compared to (a) and (c).

presented enabling fixed point stabilization with two delay times, only. In this case the choice of delay times is as follows: solid line: $\tau_1=6$; dash-dotted line: $\tau_1=6, \tau_2=4$; dotted line: $\tau_1=6, \tau_2=4, \tau_3=1.5$, and dashed line: $\tau_1=6, \tau_2=4, \tau_3=1.5$, and $\tau_4=17.7$. No (deep) notches are in the range of the system's main frequencies. Applying additionally the other two delay times only decreases the maximal real part of the eigenvalues and makes the feedback more stable. Until now all gain factors were chosen equally. The manipulation of these gains can change the characteristics of the transfer function dramatically. Using the same delay times as in Fig. 3(c) but different gain factors $k_{1a}=1.3$, $k_{1b}=0.7$, $k_{2a}=0.4$, $k_{2b}=1.0$, $k_{3a}=0.8$, $k_{3b}=0.5$, $k_{4a}=0.4$, and $k_{4b}=0.7$ yields the transfer function shown in Fig. 3(d).

With a proper choice of the gains k_{ia}, k_{ib} it is possible to match MDFC to the experimental situation. The examples presented in Fig. 3 show that this kind of filter with several delay times is different from a high-pass filter given by (4) and more flexible to be adjusted to the given control problem.

B. Colpitts oscillator

A further illustration of the MDFC approach is given by the Colpitts oscillator which is a standard example for an electronic circuit showing chaotic motion [17]. The variables correspond to voltages (U_{C_1}, U_{C_2}) and a current (I_L) within the circuit that can be described by three ordinary differential equations (ODEs):

$$C_1 \frac{dU_{C_1}}{dt} = -\alpha_F f(-U_{C_2}) + I_L + u(t),$$

$$C_2 \frac{dU_{C_2}}{dt} = (1-\alpha_F) f(-U_{C_2}) - G_0 U_{C_2} + I_L - I_0,$$

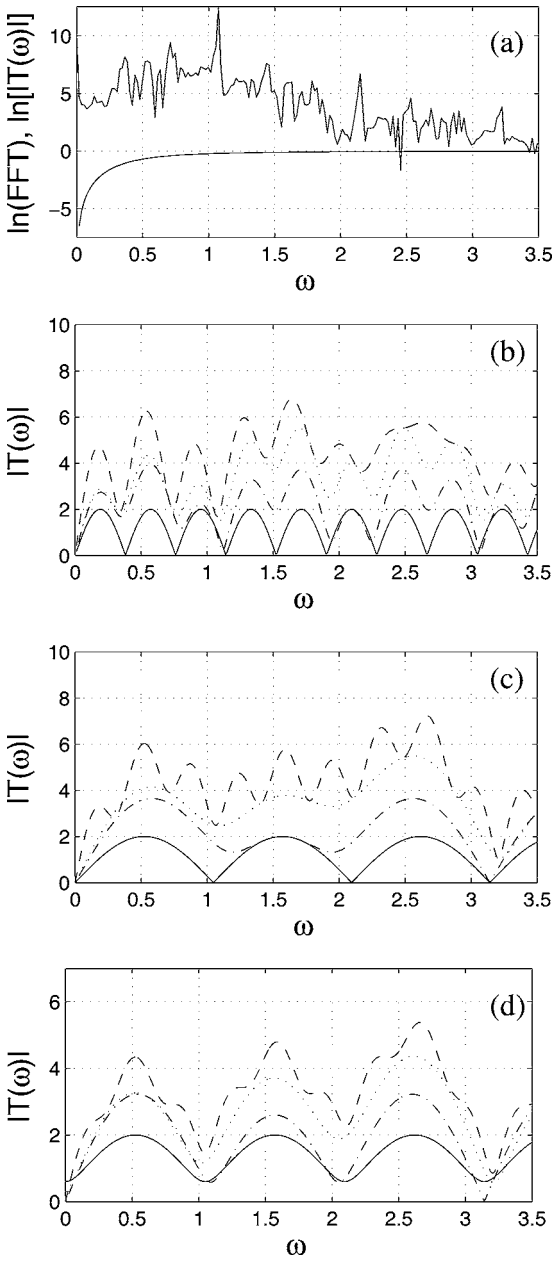

FIG. 3. (a) Fourier spectrum of the unperturbed Rössler system and transfer function of a high-pass filter with cutoff frequency $\omega_0=0.5$. (b)–(d) Transfer functions (21) for different choices of delay times and gain factors: (b) $k_i=1$, solid line: $\tau_1=16.5$, dash-dotted line: $\tau_1=16.5$ and $\tau_2=6$, dotted line: $\tau_1=16.5, \tau_2=6$, and $\tau_3=1.5$, dashed line: $\tau_1=16.5, \tau_2=6, \tau_3=1.5$, and $\tau_4=17.7$. No fixed point stabilization is possible if only the first two of these delay times are used, because of notches $[|T(\omega)|\approx 0]$ in the range of the main frequency of the free running Rössler system [compare spectrum in Fig. 3(a)]. (c) $k_i=1$, solid line: $\tau_1=6$, dash-dotted line: $\tau_1=6$, and $\tau_2=4$, dotted line: $\tau_1=6, \tau_2=4$, and $\tau_3=1.5$, dashed line: $\tau_1=6, \tau_2=4, \tau_3=1.5$, and $\tau_4=17.7$. For two or more delay times no notches are located in the range of the main frequency of the free running Rössler system. (d) Same delay times as in (c) but different gains: $k_{1a}=1.3$, $k_{1b}=0.7$, $k_{2a}=0.4$, $k_{2b}=1.0$, $k_{3a}=0.8$, $k_{3b}=0.5$, $k_{4a}=0.4$, and $k_{4b}=0.7$.

$$L\frac{dI_L}{dt} = -U_{C_1} - U_{C_2} - RI_L + U_{cc} \tag{22a}$$

with parameters $L=91\ \mu\text{H}, R=33\ \Omega$, $R_1=242\ \Omega$, $C_1=68$ nF, $C_2=68$ nF, $I_s=14.34$ fA, $U_t=0.027$ V, $\alpha_F\approx 0.99$, $U_{cc}=5$ V, $G_0=0$,

$$I_E = f(U_{BE}) = \frac{I_S}{\alpha_F}\left[\exp\left(\frac{U_{BE}}{U_t}\right)\right],$$

$$I_0 = \frac{U_{C_2} + U_{cc}}{R_1},$$

$$T = \sqrt{L\frac{C_1C_2}{C_1 + C_2}},$$

and $u=0$ in the case of the free running system. T denotes a typical time scale of the oscillator (natural period $=2\pi T$) and the feedback signal $\mathbf{u}=[u(t),0,0]$ is given by the capacitor voltage U_{C_1} as

$$u(t) = \sum_{i=1}^{4} k_i[U_{C_1}(t-\tau_i) - U_{C_1}(t)]. \tag{22b}$$

Figure 4 shows stability diagrams of the Colpitts example. As can be seen, no TDAS stabilization is possible for $\tau_1/T=\tau_2/T>2$ whereas MDFC with $\tau_1\neq\tau_2$ stabilizes the fixed point for much larger delay times [black stripes in parallel to the diagonal in Fig. 4(a)]. The heights of the peaks in Fig. 4(b) for different delay times ($\tau_1\neq\tau_2$) in parallel to the diagonal also indicate higher stability of MDFC compared to conventional TDAS ($\tau_1=\tau_2$). To demonstrate again the advantage of using several different delay times Figs. 4(c) and 4(d) show results for simulations using three delay terms at a fixed value for all gain factors ($k_1=k_2=k_3=1.35$). Regions of stability are extremely enlarged when using four delay times (actually, the whole $\tau_1/T-\tau_2/T$ plane is marked black for $\tau_3/T=3.1$, $\tau_4/T=1.32$). For the Colpitts oscillator the horizontal and vertical distance of stripes running in parallel to the diagonal in Fig. 4 equals approximately πT (i.e., half of the natural period of the Colpitts oscillator).

To investigate the gain dependence of MDFC we consider the case of three delay times, $\tau_1=\tau_2+1.6$ and $\tau_3=3.1$. This corresponds to the white dash-dotted line in Fig. 4(c). Figure 4(e) shows a stability diagram of the k-τ_2/T plane for $\tau_1=\tau_2+1.6$ and $\tau_3=3.1$. In Fig. 4(f) the corresponding stability function $\min[0,\text{Re}(\lambda)]$ is shown with a minimum of about -0.4. The larger the delay times are chosen the lower is the achieved stability of the considered fixed point but in contrast to (E)TDAS stabilization is still possible.

Figures 5(a)–5(d) show again stability diagrams for TDAS and ETDAS ($R=0.7$) control applied to the Colpitts oscillator. Similar to the results obtained for the Rössler system shown in Figs. 1(c)–1(f) the stability regions of TDAS [marked in black and gray in Figs. 5(a) and 5(b)] are enlarged by ETDAS [Figs. 5(c) and 5(d)] but remain restricted to delay times $\tau<6T$ whereas MDFC is able to stabilize the fixed point for much larger delay times.

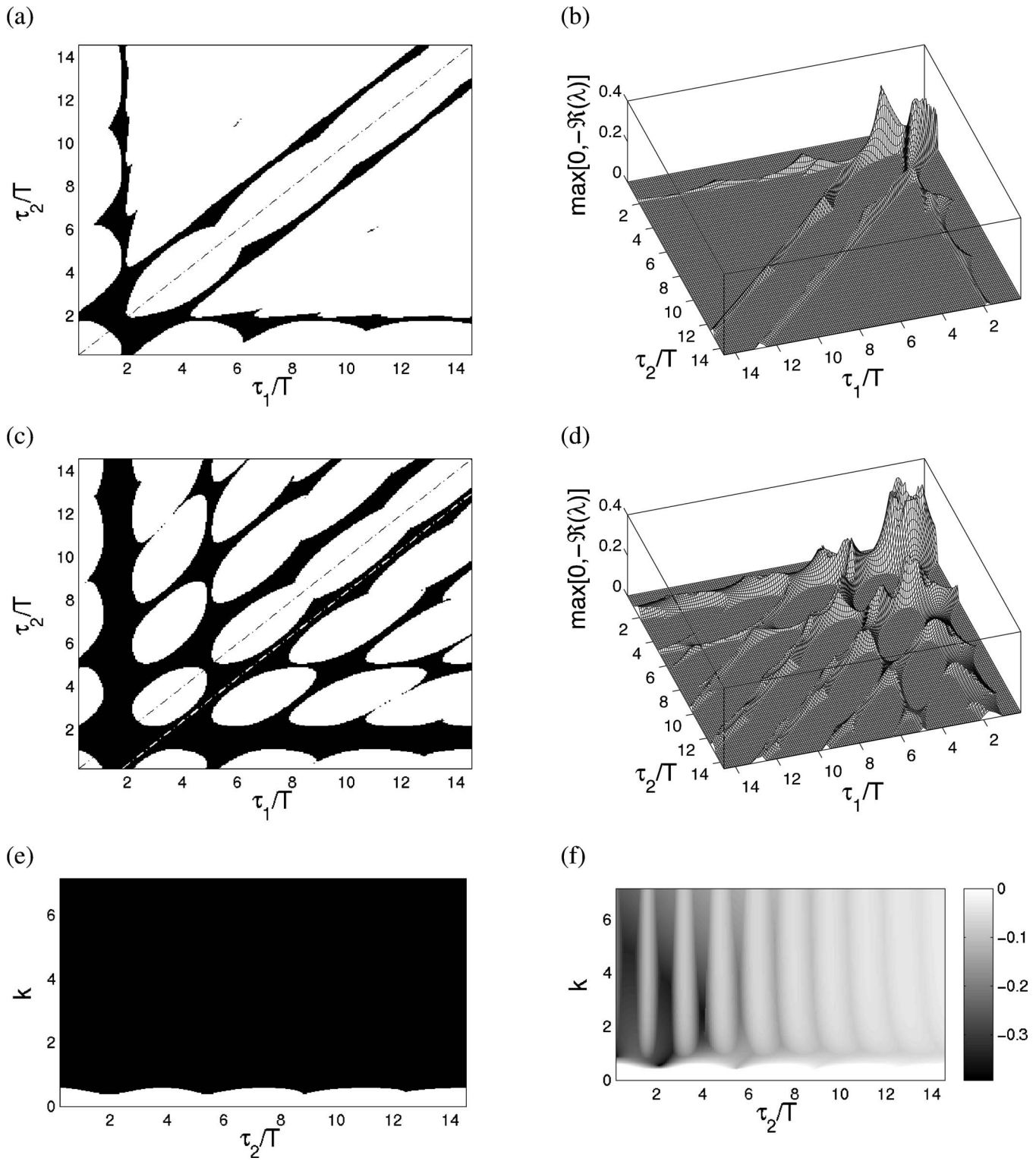

FIG. 4. Stability diagrams of the controlled Colpitts oscillator (22a) and (22b) using MDFC with (a), (b) two and (c), (d) three delay times ($k_i=1.35, \tau_3=3.1$). In (a) and (c) combinations of normalized delay times τ_1/T and τ_2/T where MDFC successfully stabilizes the fixed point are marked in black. (b) and (d) show the stability function $\max[0,-\mathrm{Re}(\lambda)]$ vs τ_1/T and τ_2/T where $\mathrm{Re}(\lambda)$ denotes the largest real part of the eigenvalues of the characteristic equation. Note that (b) and (d) are rotated compared to (a) and (c), respectively. (e) k dependence of MDFC along the white dash-dotted line shown in (c) where the control signal (22b) with $\tau_1=\tau_2+1.6$, $\tau_3=3.1$, $k_1=k_2=k_3=k$, and $k_4=0$ is applied to the Colpitts system. (f) Gray-scaled stability function $\min[0,\mathrm{Re}(\lambda)]$ vs τ_2/T for the same parameters as in (e).

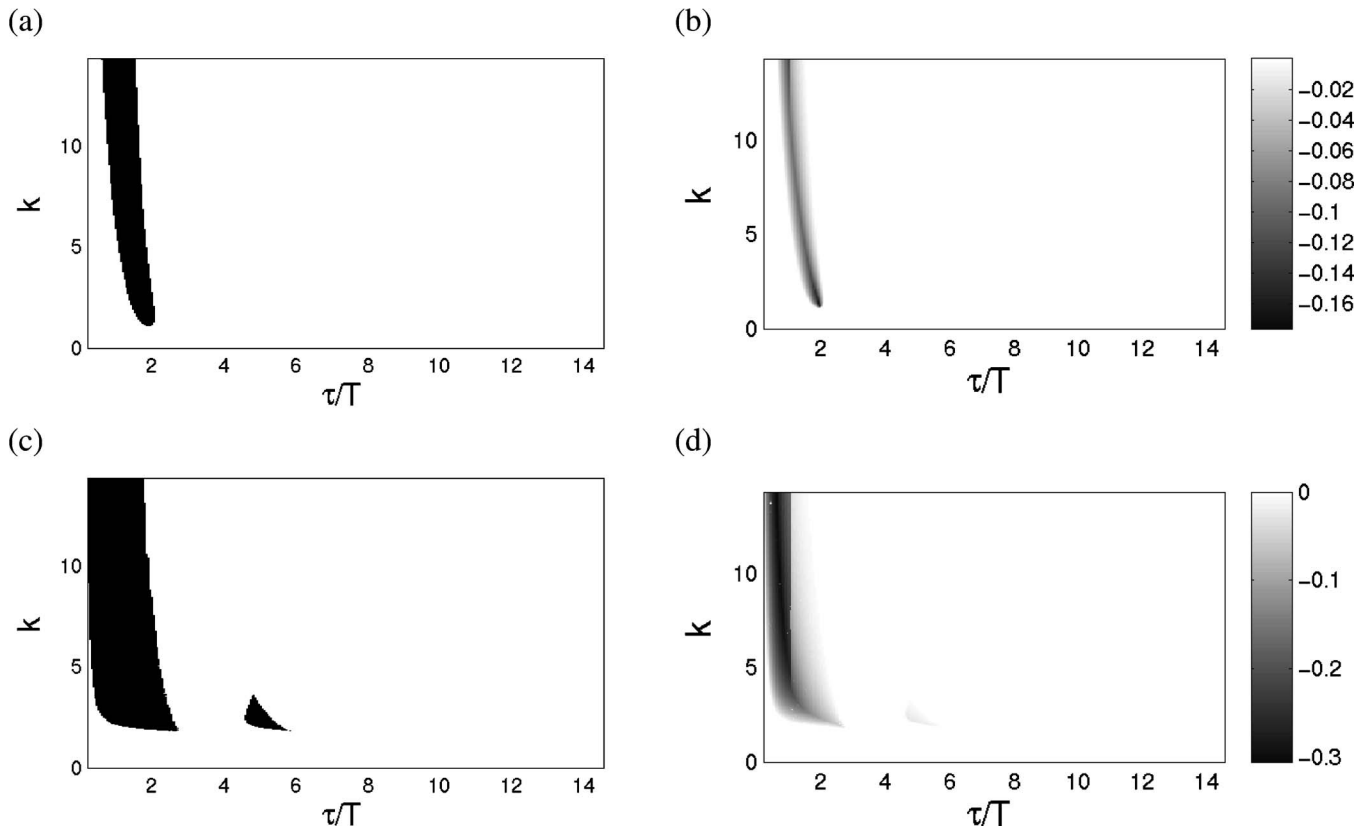

FIG. 5. Stability diagrams for (a), (b) TDAS and (c), (d) ETDAS ($R=0.7$) where the control signal (3) is applied to the Colpitts system (22a). In (a) and (c) those parameter combinations that lead to fixed point stabilization are plotted black and (b) and (d) show gray-scaled stability functions $\min[0,\mathrm{Re}(\lambda)]$ vs τ/T and k.

We shall now compare MDFC with the high pass filter (4) as a limit of ETDAS for $R\to 1,\tau\to 0$. The result for this ETDAS limit is shown in Fig. 6, where the stability function $\min[0,\mathrm{Re}(\lambda)]$ is plotted vs cutoff frequency ω_0 and feedback gain k. The stability of the feedback (represented by the largest real part of the eigenvalues of the perturbed system) is gray-scaled and the darker the gray the more stable is the feedback for the chosen parameters. The eigenvalues are calculated by standard stability analysis of the linearized perturbed vector field. One can read from this figure that the most stable real part for combinations of the cutoff frequency ω_0 and k is about -0.3. Thus, the limit cases for ETDAS ($R\to 1,\tau\to 0$) and ETDAS with a finite value of $R=0.7$ (Fig. 5) provide nearly the same stability. Both are more stable than TDAS [minimum of $\mathrm{Re}(\lambda)\approx -0.17$] but less stable than MDFC based on three delay times [minimum of $\mathrm{Re}(\lambda)\approx -0.4$], but provide for the Colpitts oscillator no stability higher than -0.3, whereas MDFC provides a value of ≈ -0.4 for moderate gain factors ($k\approx 1.5$).

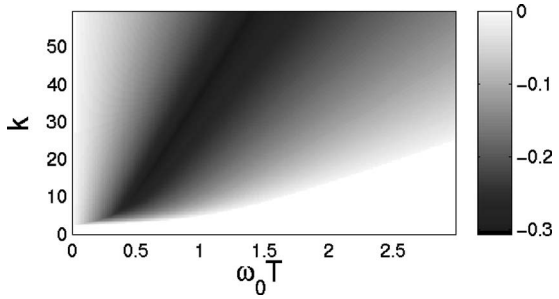

FIG. 6. Gray-scaled stability function $\min[0,\mathrm{Re}(\lambda)]$ of the Colpitts oscillator (22a) controlled using the feedback signal $\dot{u}(t)=-\omega_0 u(t)-k\dot{U}_{C_1}$. ω_0 denotes the cutoff frequency and k the gain of the high pass filter. The darker the gray the more stable is the feedback.

C. Lorenz system

Our next example is the Lorenz system

$$\dot{x} = -\sigma(x-y)+u(t),$$

$$\dot{y} = rx - y - xz,$$

$$\dot{z} = -bz + xy \tag{23a}$$

with the standard parameter values $\sigma=10$, $b=8/3$, and $r=28$. We consider here a feedback signal $\mathbf{u}=[u(t),0,0]$ depending and acting on the x variable

$$u(t) = k_1[x(t-\tau_1)-x(t)] + k_2[x(t-\tau_2)-x(t)] + k_3[x(t-\tau_3)-x(t)] + k_4[x(t-\tau_4)-x(t)]. \tag{23b}$$

The Lorenz system possesses three steady states,

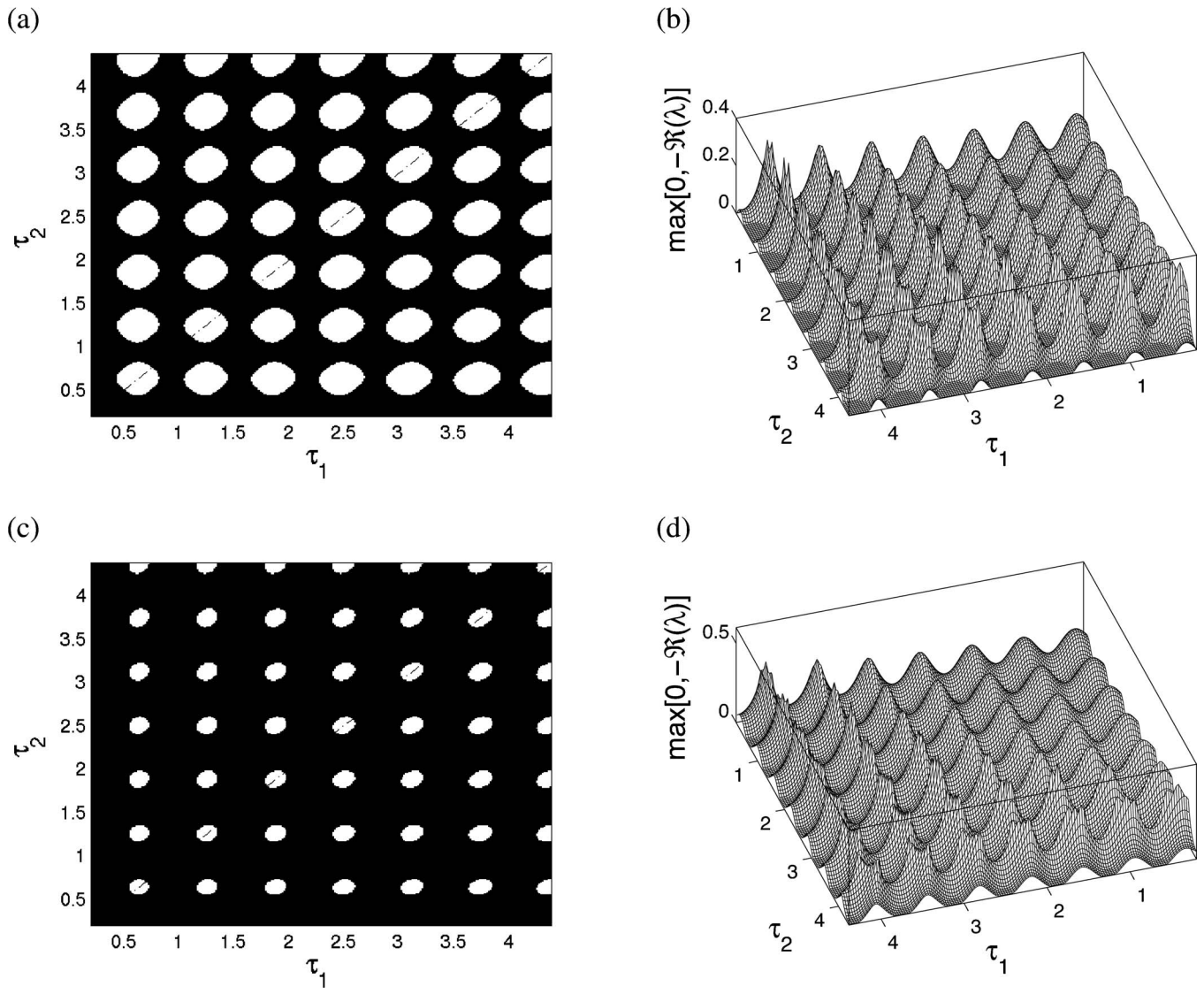

FIG. 7. Stability diagram of the controlled Lorenz system (23a) and (23b) for (a), (b) $k_1=k_2=0.7$, $k_3=k_4=0$ and (c), (d) $k_1=k_2=k_3=0.7$, $k_4=0, \tau_3=1.40$. Combinations of delay times τ_1 and τ_2 where MDFC successfully stabilizes the fixed point are plotted in black. (b), (d) Corresponding stability function $\max[0,-\mathrm{Re}(\lambda)]$ vs delay times. $\mathrm{Re}(\lambda)$ denotes the largest real part of the eigenvalues of the characteristic equation (24). Note that (a), (c) and (b), (d) show the τ_1-τ_2 plane from different perspectives.

$$\mathbf{x}_1 = \begin{bmatrix} \sqrt{b(r-1)} \\ \sqrt{b(r-1)} \\ r-1 \end{bmatrix}, \quad \mathbf{x}_2 = \begin{bmatrix} -\sqrt{b(r-1)} \\ -\sqrt{b(r-1)} \\ r-1 \end{bmatrix}, \quad \mathbf{x}_3 = \begin{pmatrix} 0 \\ 0 \\ 0 \end{pmatrix},$$

and we shall consider here the outer two $(\mathbf{x}_1, \mathbf{x}_2)$. The determinant of the characteristic matrix for the Lorenz equations is given by

$$\det[\Delta(\lambda)] = [\lambda + \sigma - u_R(\lambda)][(\lambda+1)(\lambda+b) + x_i^2] + \sigma[x_i y_i + (z_i - r)(\lambda + b)] \stackrel{!}{=} 0, \tag{24}$$

where x_i, y_i, $z_i (i \in \{1, 2\})$ denote the components of the investigated fixed points and u_R is defined in Eq. (17). Figure 7 shows stability diagrams for two [Figs. 7(a) and 7(b)] and three [Figs. 7(c) and 7(d)] delay times. In contrast to the results for the Rössler system [Fig. 1(b)] the peaks in Figs. 7(b) and 7(d) possess nearly the same height, i.e., the stabilization loses its effectiveness only slowly for increasing delay times. For the Lorenz system it is even possible to achieve steady-state stabilization with only three delay terms for any τ_1, τ_2 configuration in the range $\tau_{1,2} \in [0.2, 4.2]$ provided the third delay term is chosen appropriately (e.g., $\tau_3 = 1.55$). Here the gain factors are fixed and equal ($k_1=k_2=k_3=0.7$).

The islands of instability are separated by half of the system's natural period $T \approx 1.06$ given by the first maximum of the autocorrelation function.

Since fixed point stabilization for the Lorenz system turned out to be not too difficult (compare Fig. 7) it was no surprise that simulations with TDAS, ETDAS ($R=0.7$) and high-pass filter control were also successful with almost the same stability features (robustness).

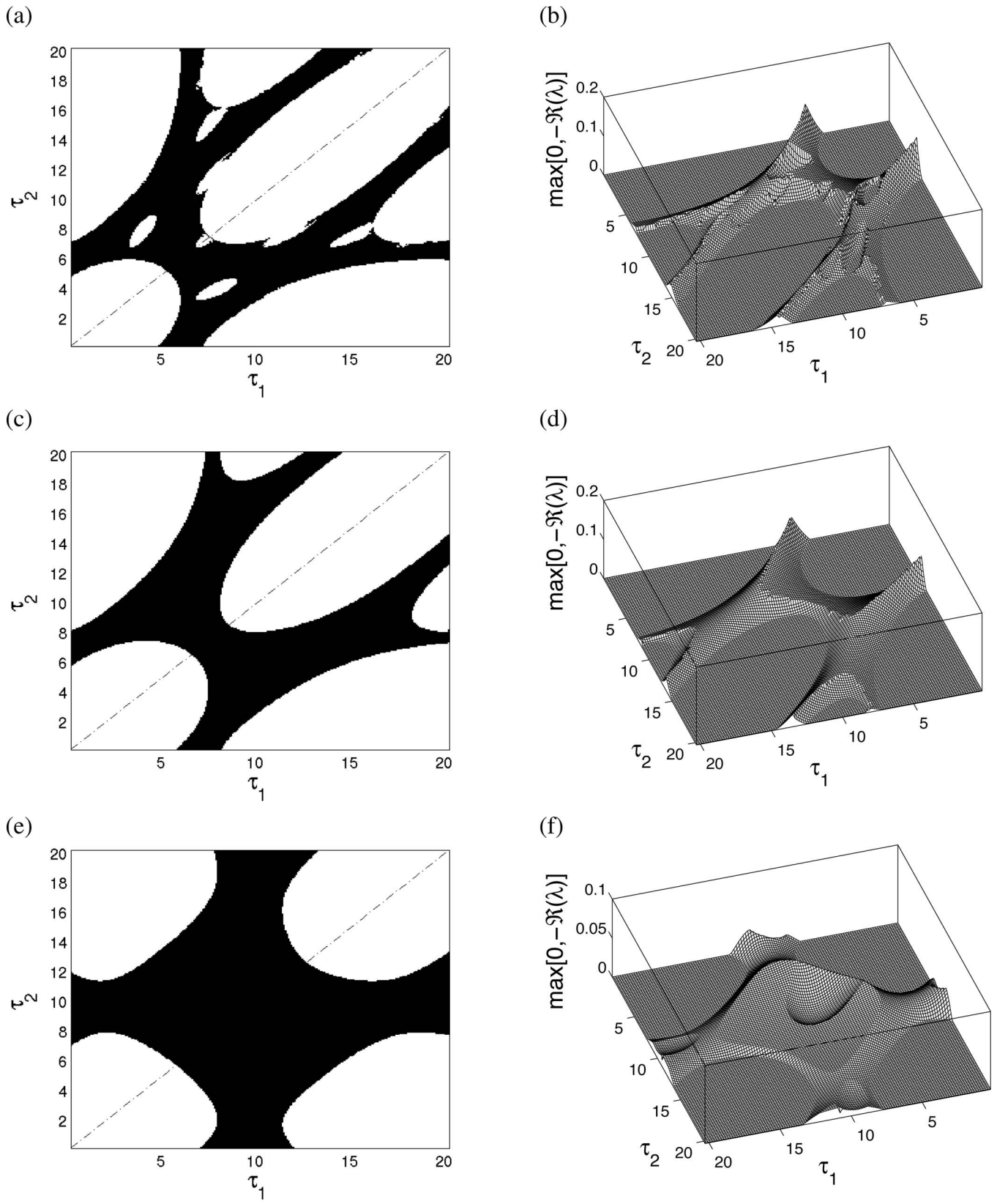

FIG. 8. Stability diagram of the controlled Baier-Sahle system (25a) and (25b) for (a),(b) $k_1=k_2=0.5$, $k_3=k_4=0$, (c),(d) $k_1=k_2=k_3=0.5$, $k_4=0$, $\tau_3=4.75$, and (e),(f) $k_1=k_2=k_3=k_4=0.5$, $\tau_3=4.75$, $\tau_4=1.43$. Combinations of delay times τ_1 and τ_2 where MDFC successfully stabilizes the considered fixed point are plotted in black. (b), (d), (f) Corresponding stability function $\max[0,-\mathrm{Re}(\lambda)]$ vs delay times τ_1 and τ_2. Re(λ) denotes the largest real part of the eigenvalues of the characteristic equation. (b), (d), and (f) are rotated compared to (a), (c), and (e).

D. Baier-Sahle system

Until now we considered three-dimensional systems. Another question is whether MDFC is able to stabilize equilibrium states for higher dimensional systems, too. To answer this question we consider a family of hyperchaotic systems introduced by Baier and Sahle [18]. These systems may be considered as higher dimensional generalizations of the Rössler system and we investigate here the five-dimensional case

$$\dot{x}_1 = -x_2 + ax_1,$$

$$\dot{x}_2 = x_1 - x_3 + u,$$

$$\dot{x}_3 = x_2 - x_4,$$

$$\dot{x}_4 = x_3 - x_5,$$

$$\dot{x}_5 = \epsilon + bx_5(x_4 - d) \tag{25a}$$

that generates for $a=0.28$, $b=4$, $d=2$, and $\epsilon=0.1$ a chaotic attractor with a correlation dimension $D_2 \approx 4.17$ when running without control ($u=0$). The control signal applied reads

$$u(t) = \sum_{i=1}^{4} k_i[x_2(t-\tau_i) - x_2(t)] \tag{25b}$$

and the fixed point we intend to stabilize is located at $\mathbf{x} = (c, ac, c, ac, c)$ with

$$c = \frac{d}{2a} - \sqrt{\frac{d^2}{4a^2} - \frac{\epsilon}{ba}}.$$

Figure 8 shows stability diagrams for MDFC control with two [Figs. 8(a) and 8(b)], three [Figs. 8(c) and 8(d)], and four [Figs. 8(e) and 8(f)] delay times. Within the stability regions marked in black in Fig. 8 little islands of instability appear where the feedback consisting of two delay terms cannot achieve stabilization of the equilibrium state. These islands of instability disappear if three or more delay times are used, resulting in an enlargement of the stability region. Here the black stripes are running in parallel to the diagonal in the τ_1-τ_2 plane at a horizontal and vertical distance of one period $T \approx 11.3$ of the natural oscillations (first maximum of the autocorrelation function).

Simulations with TDAS, ETDAS ($R=0.7$), and high-pass filter control (ETDAS for $R \to 1$ and $\tau \to 0$) confirmed the general observation that MDFC provides extended stability regions with more stable control or equal stability.

V. CONCLUSION

Numerical simulations for different chaotic dynamical systems show that *multiple delay feedback control* (MDFC) is superior to TDAS and ETDAS in terms of stability and flexibility when used for stabilizing unstable steady states. Linear stability analysis clearly indicates that MDFC not only provides solutions that are more stable (in terms of negative real parts of relevant eigenvalues) but also enables stabilization for larger delay times where (E)TDAS may fail completely. Simulations with different systems show that the efficiency of MDFC increases when including more independent delay times in the feedback loop. To understand this feature it is useful to analyze MDFC in the frequency domain where it corresponds to transfer functions that depend on delay times and gain factors. The more delay times are involved the more flexible this transfer function can be adjusted to the dynamics in order to suppress specific frequency components. Since many extended systems are internally coupled with different delays we expect the stabilizing effect of multiple delay feedback to be relevant for this class of systems, too.

ACKNOWLEDGMENTS

We thank our colleagues at the Third Physical Institute for encouraging and stimulating discussions about delay control.

[1] H. G. Schuster (ed.), *Handbook of Chaos Control* (Wiley-VCH, Weinheim, 1999); T. Kapitaniak (ed.), *Controlling Chaos* (Academic Press, London, 1996).
[2] E. Ott, C. Grebogi, and J. Yorke, Phys. Rev. Lett. **64**, 1196 (1990).
[3] E. R. Hunt, Phys. Rev. Lett. **67**, 1953 (1991).
[4] K. Myneni, T. A. Barr, N. J. Corron, and S. D. Pethel, Phys. Rev. Lett. **83**, 2175 (1999).
[5] K. Pyragas, Phys. Lett. A **170**, 421 (1992).
[6] W. Just, H. Benner, and E. Reibold, Chaos **13**, 259 (2003).
[7] A. Namajunas, K. Pyragas, and A. Tamasevicius, Phys. Lett. A **204**, 255 (1995).
[8] J. E. S. Socolar, D. W. Sukow, and D. J. Gauthier, Phys. Rev. E **50**, 3245 (1994).
[9] D. W. Sukow, M. E. Bleich, D. J. Gauthier, and J. E. S. Socolar, Chaos **7**, 560 (1997).
[10] A. Chang, J. C. Bienfang, G. M. Hall, J. R. Gardner, and D. J. Gauthier, Chaos **8**, 782 (1998).
[11] D. J. Gauthier, Opt. Lett. **23**, 703 (1998).
[12] J. E. S. Socolar and D. J. Gauthier, Phys. Rev. E **57**, 6589 (1998).
[13] J. N. Blakely, L. Illing, and D. J. Gauthier, Phys. Rev. Lett. **92**, 193901 (2004).
[14] A. Ahlborn and U. Parlitz, *Proceedings of the Experimental Chaos Conference 8 (ECC8)*, Florence 14.6. - 17.6.2004, AIP Conf. Proc. 742, 241 (2004).
[15] A. Ahlborn and U. Parlitz, Phys. Rev. Lett. **93**, 264101 (2004).
[16] J. K. Hale, Theory of Functional Differential Equations, *Appl. Math. Sci. 3* (Springer Verlag, Berlin, 1977).
[17] O. de Feo, G. M. Maggio, and M. P. Kennedy, Int. J. Bifurcation Chaos Appl. Sci. Eng. **10**(5), 935 (2000).
[18] G. Baier and S. Sahle, Phys. Rev. E **51**(4), R2712 (1995).

[19] All stability diagrams shown in this article are computed for $\tau_i > 0.2$, i.e., borders with $\tau_1=0$ or $\tau_2=0$ are not included. Therefore, TDAS control with a single delay time occurs in these plots only along the diagonal $\tau_1=\tau_2$ in the τ_1-τ_2 plane using the gain factor $k=\Sigma k_i$. Extrapolating the τ_1-τ_2 stability plot to the cases $\tau_1=0$ or $\tau_2=0$ leads to TDAS control with gains $k=k_2$ or $k=k_1$. The stability results for these different gains can be obtained from the provided TDAS control plots Figs. 1(d) and 5(b) taking into account the effective gain values.